Published in final edited form as:
Circ Res. 2013 August 16; 113(5): . doi:10.1161/CIRCRESAHA.113.301792.

A Role for the Endothelium in Vascular Calcification

Yucheng Yao[1], **Medet Jumabay**[1], **Albert Ly**[1], **Melina Radparvar**[1], **Mark R. Cubberly**[1], and **Kristina I. Boström**[1,2]

[1]Division of Cardiology, David Geffen School of Medicine at UCLA, Los Angeles, CA 90095-1679

[2]Molecular Biology Institute, UCLA

Abstract

Rationale—Vascular calcification is a regulated process that involves osteoprogenitor cells and frequently complicates common vascular disease such as atherosclerosis and diabetic vasculopathy. However, it is not clear if the vascular endothelium has a role in contributing osteoprogenitor cells to the calcific lesions.

Objective—To determine if the vascular endothelium contributes osteoprogenitor cells to vascular calcification.

Methods and Results—In this study, we use two mouse models of vascular calcification, mice with gene deletion of matrix Gla protein (MGP), a BMP-inhibitor, and *Ins2*$^{Akita/+}$ mice, a diabetes model. We show that enhanced bone morphogenetic protein (BMP) signaling in both types of mice stimulates the vascular endothelium to contribute osteoprogenitor cells to the vascular calcification. The enhanced BMP signaling results in endothelial-mesenchymal transitions and the emergence of multipotent cells, followed by osteoinduction. Endothelial markers co-localize with multipotent and osteogenic markers in calcified arteries by immunostaining and fluorescence-activated cell sorting. Lineage tracing using *Tie2-Gfp* transgenic mice supports an endothelial origin of the osteogenic cells. Enhancement of MGP expression in *Ins2*$^{Akita/+}$ mice, as mediated by an *Mgp* transgene limits the generation of multipotent cells. Moreover, MGP-depleted human aortic endothelial cells *in vitro* acquire multipotency rendering the cells susceptible to osteoinduction by BMP and high glucose.

Conclusions—Our data suggest that the endothelium is a source of osteoprogenitor cells in vascular calcification that occurs in disorders with high BMP activation such as deficiency of BMP inhibitors and diabetes.

Keywords

Vascular calcification; endothelium; matrix Gla protein; bone morphogenetic protein; endothelial-mesenchymal transition

INTRODUCTION

Vascular calcification is a frequent complication of vascular disease such as diabetes mellitus, renal disease and atherosclerosis, and is associated with an increased risk of

Address correspondence to: Dr. Yucheng Yao, Division of Cardiology, David Geffen School of Medicine at UCLA, 10833 Le Conte Ave, CHS A2-237, Box 951679, Los Angeles, CA 90095-1679, Tel: 1 310-794-4417, Fax: 1 310-206-8553., yyao@mednet.ucla.edu. Dr. Kristina I. Boström, Division of Cardiology, David Geffen School of Medicine at UCLA, 10833 Le Conte Ave, CHS A2-237, Box 951679, Los Angeles, CA 90095-1679, Tel: 1 310-794-4417, Fax: 1 310-206-8553., kbostrom@mednet.ucla.edu.

DISCLOSURES
None.

cardiovascular and all-cause mortality [1]. It is a regulated process with strong similarities to bone formation driven by osteochondrogenic progenitor cells [1]. Vascular medial cells functioning as adult mesenchymal stem cells or smooth muscle cells (SMCs) transdifferentiating into multipotent cells are believed to be the major contributors of such progenitor cells [1, 2].

Interestingly, endothelial cells (ECs) have been reported to contribute osteoblastic cells in fibrodysplasia ossificans progressiva (FOP), a rare genetic disorder linked to mutations in the activin receptor-like kinase 2 (ALK2), a receptor for bone morphogenetic protein 4 (BMP4) [3]. FOP is characterized by the development of soft tissue masses outside major vessels, in which ECs undergo endothelial-mesenchymal transitions (EndMT) and contribute cells to the ectopic ossification [4]. Furthermore, prostate tumor endothelial cells have been shown to undergo mesenchymal-like transitions and osteochondrogenic differentiation [5], mitral valve leaflets contain ECs with osteogenic potential [6], and high glucose can induce transdifferentiation into chondrocyte-like cells in human aortic ECs [7]. However, it is not known whether the arterial endothelium can act as a source of osteoprogenitor cells in vascular calcification, a frequent complication of vascular disease.

BMP signaling is known to promote vascular calcification, and others and we have reported that limiting vascular BMP signaling decreases both atherosclerotic lesion and diabetic medial calcification [8–11]. Endothelial expression of BMP2 and 4 is highly responsive to pathological stimuli such as disturbed flow, increased oxidative stress, inflammation, and hyperglycemia [12, 13], which may contribute to calcification [1, 9]. In diabetes, there is also a differential induction of BMP2 and 4 in the vascular wall; BMP2 is induced in the vascular media where it may have an osteoinductive effect, whereas BMP4 is preferentially induced in the endothelium [9]. Activation of BMP signaling leads to an induction of BMP inhibitors [14, 15], which provide negative feedback regulation. Matrix Gla protein (MGP), which directly binds and inhibits BMP2, 4 and 7 [16–18], is readily induced in response to BMP activation in the vascular wall. Loss of MGP causes excess BMP activity, extensive media calcification and early death due to vascular rupture [19], whereas the presence of a *Mgp* transgene increases the MGP induction in response to BMP, enhancing the regulation of the BMP activity [8, 9].

Here, we demonstrate that endothelium may be a source of multipotent osteoprogenitor cells in vascular calcification that occurs in the setting of high BMP activity in mice lacking MGP and in diabetic mice with high vascular BMP expression.

METHODS

See Supplemental Material for further details on fluorescence-activated cell sorting (FACS) analysis, immunostaining, transmission electron microscopy (TEM), and analytical procedures.

Animals

Mgp$^{+/-}$ mice on C57BL/6J background were obtained from Dr. Cecilia Giachelli (University of Washington, Seattle) with the permission of Dr. Gerard Karsenty (Columbia University, New York), and have been backcrossed more than 10 times. *Ins2*$^{Akita/+}$ mice (strain C57BL/6-Ins^{Akita}/J, stock # 003548), which are heterozygous for a mutation in one allele of the insulin-2 gene [20, 21] were obtained from the Jackson Laboratory. *Mgp*$^{tg/wt}$ mice, generated in our laboratory on a C57BL/6J background [22], were crossed with *Ins2*$^{Akita/+}$ mice to generate *Mgp*$^{tg/wt}$;*Ins2*$^{Akita/+}$ mice. Heterozygous *Mgp*$^{tg/wt}$ mice were used because the phenotype was apparent in *Mgp*$^{tg/wt}$ mice, and a low birth rate made it difficult to obtain hemizygous *Mgp*$^{tg/tg}$ mice [22]. *Tie2-Gfp* transgenic (tg) mice (strain Tg(TIE2GFP)287Sato/J, stock #

003658), which express Green Fluorescent Protein (GFP) under the control of the endothelial-specific *Tie2* promoter, were obtained from the Jackson Laboratory. Genotypes were confirmed by PCR [2, 22, 23], and experiments were performed with generation F4–F6. All mice were fed a standard chow diet (8604 Teklad Rodent Diet, Harlan Laboratories). *Mgp*$^{-/-}$ and *Mgp*$^{-/-}$*;Tie2-Ggp*tg mice were used for experiments at 4 weeks of age, whereas *Ins2*$^{Akita/+}$, *Mgp*$^{tg/wt}$;*Ins2*$^{Akita/+}$ and *Ins2*$^{Akita/+}$*;Tie2-Ggp*tg mice were used at 35–40 weeks of age. Only male mice with the Ins2-Akita mutation were used for experiments, and littermates were used as controls. The investigation conformed to the *Guide for the Care and Use of Laboratory Animals* published by the US National Institutes of Health (NIH Publications No. 85–23, revised 1996), and had been reviewed and approved by the Institutional Review Board of the University of California, Los Angeles.

Cell culture and SiRNA transfection

Human aortic endothelial cells (HAECs) were prepared and cultured as described [15, 24]. Transient transfections of HAEC with siRNA were performed with Lipofectamine™2000 (Invitrogen) using 60 nM siRNA as described [15]. Three separate siRNAs to each protein (Silencer® predesigned siRNA, Ambion) and scrambled siRNA with the same nucleotide content were tested. The siRNA that provided the most efficient inhibition (90–95%), as determined by real-time PCR and immunoblotting or immunostaining, was used for experiments. Silencer® predesigned siRNAs were obtained for MGP, Cbfa1, and SM22α. Treatments were initiated 12–24 hours after the start of transfection, after removal of the transfection agent. For treatment, BMP2, BMP4, Noggin (all from R&D Systems), glucose, and osteogenic medium were added as indicated in the text.

FACS

FACS was performed as detailed in Supplemental Methods.

RNA analysis

RT-PCR and real-time PCR were performed as described [15]. GAPDH was used as a control gene. Primers and probes for CD31, VE-cadherin, Flk-1, Sox2, Nanog, Oct3/4, Cbfa1, and Osterix were obtained from Applied Biosystems as part of TaqMan Gene Expression Assays.

Immunoblotting

Immunoblotting was performed as described [25, 26]. Equal amounts of tissue or cellular protein were used. Tissues were collected at 4 weeks for *Mgp*$^{-/-}$ mice and controls, and at 35–40 weeks for mice with the *Ins2*^{Akita} mutation and controls. Blots were incubated with specific antibodies to CD31 (300 ng/ml; Cell Signaling Technology); VE-cadherin (400 ng/ml; Santa Cruz Biotechnology); Flk-1 (200 ng/ml; Santa Cruz Biotechnology); Sox2 (200 ng/ml; Cell Signaling); Nanog (400 ng/ml; BD Pharmingen and eBioscience); Oct3/4 (200 ng/ml; R&D Systems); Cbfa1 (500 ng/ml; Oncogene Research Products); Osterix); SM22α (200 ng/ml; Santa Cruz Biotechnology) and αSMA (200 ng/ml; R&D Systems). β-Actin (1:5,000 dilution; Sigma-Aldrich) was used as loading control.

Immunostaining

The tissues were collected at 4 weeks for *Mgp*$^{-/-}$ mice and 35–40 weeks for mice with the *Ins2*^{Akita} mutation, and the proximal descending aorta was used for tissue sections (Supplemental Figure I, left). We did not detect any particular areas that consistently showed more calcification than others in the mice that were included in this study. The calcification in the *Mgp*$^{-/-}$ mice was very extensive and uniform (Supplemental Figure I, right). The tissue sections were fixed in 4% paraformaldehyde and processed as described [9]. Cultured

cells were grown in chamber slides and fixed in 4% paraformaldehyde for 30 minutes, permeabilized with 0.1% Triton X-100, and blocked with 1% goat serum and 1% bovine serum albumin in Tris-buffered saline, and incubated overnight. The cells were immunostained using the same protocol as the tissues.

Immunofluorescence was performed as described in Supplemental Methods [9]. We used specific antibodies for CD31 (Millipore), vWF (Dako), Cbfa1 and Osterix (Oncogene Research Products), SM22α (Santa Cruz Biotechnology), αSMA and Oct3/4 (R&D Systems), Sox2 (Cell Signaling), Nanog (BD Pharmingen and eBioscience), GFP (Abcam), and MGP (Dr. Reidar Wallin, Wake Forest University). The nuclei were stained with 4′,6-Diamidino-2-Phenylindole (DAPI) (Sigma-Aldrich) [24]. Non-specific IgG was included as a primary antibody control in all experiments, where it showed no significant staining, which has been included in selected figures.

TEM

Aortic tissue samples were analyzed by TEM as described in Supplemental Methods.

Histochemical staining

Histochemical staining for alkaline phosphatase activity and mineral (Alizarin Red and Von Kossa) was performed as previously described [9].

Analytical procedures

Samples were analyzed as described in Supplemental Methods.

Statistical analysis

Data were analyzed for statistical significance by two-way analysis of variance with post hoc Tukey's analysis using the GraphPad Instat® 3.0 software (GraphPad Software, San Diego, CA). P-values less than 0.05 were considered significant. All experiments were repeateda minimum of three times.

RESULTS

Endothelial origin of osteogenic cells in $Mgp^{-/-}$ calcified aortas

To determine whether the endothelium contributes osteoprogenitor cells to vascular calcification, we first compared the aortic endothelium in wild type and $Mgp^{-/-}$ mice, a well-known model of vascular calcification [19]. These mice are known to be tachycardic [19] with a very high pulse wave velocity in the aorta at rest [27], presumably from the dramatic increase in aortic calcium [8], and endothelial dysfunction as evidenced by minimal inflammatory response to hyperlipidemia [8] and the formation of arteriovenous malformations [17]. In $Mgp^{-/-}$ mice, the endothelium was highly abnormal as visualized by phase contrast and transmission electron microscopy; a mixture of cells largely replaced normal ECs, including chondroblast-like cells (Figure 1A, the magnification is the same in all panels). Occasionally, EC-like cells were detected that appeared to have detached from the internal elastic lamina (IEL) and were surrounded by abnormal matrix (Figure 1A, bottom panels). The abnormalities were associated with increased aortic expression of EC lineage markers CD31, VE-cadherin and fetal liver kinase 1 (Flk-1), as determined by real-time PCR and immunoblotting (Figure 1B). Furthermore, CD31 and von Willebrand factor (vWF) expression was detected deep in the calcified media (Figure 1B), and immunostaining showed co-expression of CD31 and vWF, respectively, with osteogenic markers core binding factor alpha 1 (Cbfa1) and Osterix (Figure 1C). The $Mgp^{-/-}$ aortas contained about 28.8% cells that double-stained for CD31 and Cbfa1, as determined by

FACS after dispersion of aortic cells (Figure 1D) and exclusion of CD45+ cells, which may represent CD31+ leukocyte populations. The efficiency of the CD45 pre-sorting was checked with FACS (Supplemental Figure II). Cells that co-expressed CD31 and a bone marker also appeared to penetrate into the media (Figure 1E).

To confirm the endothelial origin of the osteogenic cells, we performed lineage tracing as described [3]. We crossed *Tie2-Gfp transgenic* (*tg*) reporter mice with $Mgp^{+/-}$ mice to obtain $Mgp^{-/-}$*;Tie2-Gfp*tg mice, in which GFP is expressed under the control of the endothelial-specific Tie2 promoter. Immunostaining revealed GFP-positive cells in the calcified aortic tissue of the $Mgp^{-/-}$*;Tie2-Gfp*tg mice (Figure 1F). Furthermore, staining with anti-Cbfa1 and Osterix antibodies revealed GFP-positive cells that co-expressed Cbfa1 and Osterix (Figure 1G). GFP was only detected in the aortic endothelium in the *Tie2-Gfp*tg control mice.

Multipotent marker expression in $Mgp^{-/-}$ endothelium

MGP is an efficient inhibitor of BMP4 [16], which can activate the ALK2 receptor and promote EndMT in ECs [3]. Therefore, we examined expression of multipotent markers Sox2, Nanog and Oct3/4 in the $Mgp^{-/-}$ aortas. The results revealed an increase of all 3 markers by immunoblotting (Figure 2A, left). The multipotent markers were detected in the cell nuclei by immunostaining, whereas the EC marker CD31 was found in the cell membranes of the same cells (Figure 2A, right). We also examined multipotent markers in the aortas of $Mgp^{-/-}$*;Tie2-Gfp*tg mice. The results confirmed the increase in Sox2, Nanog and Oct3/4 expression by immunoblotting (Figure 2B, left). Sox2, Nanog and Oct3/4 were localized in the nuclei of GFP-expressing cells of Tie2-positive lineage by immunostaining (Figure 2B, right). Cells that only stained for the stem cell markers were noted in both $Mgp^{-/-}$ and $Mgp^{-/-}$*;Tie2-Gfp*tg aortas (Figure 2A, B) and may represent SMC-like or other multipotent cells. FACS after aortic cell dispersion and exclusion of CD45+ cells showed that about 32.1% co-stained for CD31 and Sox2 (Figure 2C). Together, the results from $Mgp^{-/-}$ and $Mgp^{-/-}$*;Tie2-Gfp*tg mice suggested that MGP-deficiency promotes multipotency in ECs.

Time course of multipotent and osteogenic marker expression in $Mgp^{-/-}$ aorta

To better understand the time course of the aortic changes, we collected aortas from $Mgp^{-/-}$ mice on postnatal day (P)2, 4, 6, 8, 10, 15, 20, and 30, and examined the aortic tissues by H&E staining, real-time PCR and immunostaining. The H&E staining showed mild abnormalities on P8, and gross calcification on P15–30, which appeared to start on the endothelial side of the vessel wall (Figure 3A, see Supplemental Figure III for higher magnification). Real-time PCR showed that expression of EC markers CD31 and VE-cadherin increased as early as P4 in the $Mgp^{-/-}$ mice, and peaked at P15 (Figure 3B). The expression of Sox2, Nanog and Oct3/4 increased on P4–6 and peaked on P15 similar to the EC markers, whereas the expression of Cbfa1 and Osterix increased on P8 and had not reached a clear peak on P30 (Figure 3B). The expression of all markers was unchanged in the wild type mice. The time course of MGP expression in wild type mice was similar to that of the EC and multipotency markers in the $Mgp^{-/-}$mice, whereas the BMP4 expression was similar in both mice (Figure 3B). MGP was not detected in the $Mgp^{-/-}$ mice as expected. Immunostaining revealed mild CD31 expression in the media of $Mgp^{-/-}$ mice on P6, which increased through P30 (Figure 4A). Sox2 and Osterix expression appeared on P8 and P10, respectively, and increased through P30 (Figure 4B, C). No significant change in CD31 expression was detected in the wild type endothelium, and Sox2 or Osterix were not detected. Overall, the data support that CD31 and the multipotency markers increase prior to the bone markers, suggesting a temporal relationship. Interestingly, the finding that the expression pattern of CD31 and Sox2 resembles that of MGP in the wild type mice suggests that MGP is required during this time period to promote EC differentiation.

Endothelial origin of osteogenic and multipotent cells in aortas of diabetic Ins2$^{Akita/+}$ mice

We previously showed increased aortic BMP activity in diabetic *Ins2*$^{Akita/+}$ mice associated with aortic osteogenesis and calcium accumulation [9]. These mice are known to develop diabetic cardiomyopathy but heart rate and blood pressure remains largely unchanged [28, 29]. In addition, there were no significant differences in serum phosphate and total cholesterol between wild type and *Ins2*$^{Akita/+}$ mice (Supplemental Table I).

To determine whether the endothelium was a source of multipotent cells in the *Ins2*$^{Akita/+}$ mice, we first demonstrated expression of CD31 and vWF in areas of calcification in the vascular media (Figure 5A). Immunostaining revealed co-expression of CD31 and vWF with Cbfa1 and Osterix in the calcified areas (Figure 5B), and FACS analysis showed that 19.2% of the aortic cells double-stained for CD31 and Cbfa1 after exclusion of CD45+ cells (Figure 5C). The *Ins2*$^{Akita/+}$ mice were then crossed with the *Tie2-Gfp*tg mice for lineage tracing. When examining the aortas of the *Ins2*$^{Akita/+}$*;Tie2-Gfp*tg mice, we detected GFP-positive cells in the endothelium and the media (Figure 5D), which co-expressed Cbfa1 and Osterix (Figure 5E), suggesting that the osteogenic cells were EC-derived. The aortic expression of Sox2, Nanog, and Oct3/4 was also increased in both *Ins2*$^{Akita/+}$ and *Ins2*$^{Akita/+}$*;Tie2-Gfp*tg mice, as determined by immunoblotting (Figure 6A), and immunostaining (Figure 6B, C). FACS analysis showed that 21.5% of the cells co-expressed CD31 and Sox2 after exclusion of CD45+ cells (Figure 6D).

Enhanced MGP expression limits multipotency in aortas of Ins2$^{Akita/+}$ mice

Our previous study showed that enhanced MGP expression limited BMP activity and aortic calcification when *Ins2*$^{Akita/+}$ mice were crossed with MGP transgenic (*Mgp*$^{tg/wt}$) mice [9]. We examined whether the enhanced MGP expression also limited multipotent marker expression in *Ins2*$^{Akita/+}$*;Mgp*$^{tg/wt}$ mice. The results revealed reductions in Sox2, Nanog, and Oct3/4 as determined by real-time PCR and immunoblotting (Figure 6E, F), supporting that the enhanced aortic expression of MGP also reduced multipotency in the diabetic aortas. Immunostaining showed that increased MGP limited CD31 expression to the endothelium (Figure 6G).

Endothelial cells acquire multipotency and susceptibility to osteoinduction after depletion of MGP

To examine the effect of loss of MGP on multipotency *in vitro*, HAECs were transfected with MGP siRNA or scrambled control siRNA (SCR). More than >99.5% of the HAECs expressed CD31 by FACS (data not shown). The siRNA transfection decreased MGP protein levels to <10–20% of normal levels as shown by immunostaining after 20–24 hours (Supplemental Figure IV). We also combined the siRNA transfection with treatment of the cells with BMP4 (40 ng/ml), Noggin (a BMP inhibitor) (200 ng/ml), or BMP4 and Noggin, added 12 hours after the transfection. The results showed that expression of Sox2, Nanog, and Oct3/4 increased after MGP depletion, as determined by immunoblotting (Figure 7A, lanes 1–2). BMP4 further increased expression of Sox2, Nanog and Oct3/4, whereas Noggin abolished the marker expression (Figure 7A, lanes 3–6). Added together, BMP4 and Noggin were similar to control (Figure 7A, lanes 7–8). We confirmed that BMP4 increased multipotency in MGP-depleted HAEC by FACS analysis. Co-expression of the stem cell markers SSEA-3 and SSEA-4, and CD31 was observed in MGP-depleted HAECs (Figure 7B, left). BMP4 increased the population of SSEA-3+/CD31+ cells from 18.9% to 57.1%, and the population of SSEA-4+/CD31+ cells from 22.8% to 60.1% (Figure 7B, right).

To test for osteogenic differentiation in MGP-depleted HAECs, we treated with osteogenic medium, BMP2 (200 ng/ml), or a combination of osteogenic medium and BMP2 for 4 days starting the day after transfection. Alternatively, we replaced the osteogenic medium with

glucose (22 nM) in order to mimic hyperglycemia. Expression of Sox2, Nanog and Oct3/4 increased after MGP depletion, but decreased when the osteoinduction was strongly promoted by the combination of BMP2 and osteogenic medium or glucose, as determined by immunoblotting (Figure 7C & E, top 3 panels). Expression of the osteogenic markers Cbfa1 and Osterix, as well as the early smooth muscle cell (SMC) markers SM22α and α-SM actin (αSMA) increased in all three conditions (Figure 7C& E , bottom panels). Interestingly, expression of SM-myosin heavy chain (SM-MHC), a late SMC marker, was not detected in any of the samples (Figure 7C& E , bottom panels). Alkaline phosphatase (ALP) activity, an early osteogenic marker, and calcium accumulation, a late osteogenic marker, increased in the MGP-depleted HAECs after 7 and 14 days of treatment, respectively, as determined by ALP and mineral staining (Alizarin Red and Von Kossa) (Figure 7D & F). Altogether, the results are consistent with the *in vivo* experiments, and support that endothelial MGP depletion may cause multipotency and osteoinduction.

SM22α expression is not required for expression of osteogenic markers in endothelial cells

Speer et al. [2] recently reported that osteochondrogenic cells in $Mgp^{-/-}$ aortas transdifferentiate from vascular SMCs based on lineage tracing using *SM22α*-Cre;*R26R-LacZ* mice. Sun et al. [30] similarly used *SM22α*-Cre mice to specifically delete Cbfa1 (Runx2) in SM22α-expressing cells, and concluded that SMC-derived Cbfa1 regulated vascular calcification. Although SM22α is considered an early marker of SMCs, it is also expressed in myofibroblasts, pericytes, and after EndMT [31–33]. To determine if SMC markers were induced in the MGP-deficient ECs, we co-stained aortas from $Mgp^{-/-}$ and $Ins2^{Akita/+}$ mice with antibodies to CD31 and SM22α or αSMA. The results showed co-expression of CD31 and SM22α or αSMA in both aortas (Figure 8A). We then tested if SM22α was required for osteoinduction in HAECs *in vitro*, and conversely, if Cbfa1 was required for expression of early SMC markers. HAECs were transfected with SCR or MGP siRNA, and MGP siRNA was co-transfected with SM22α or Cbfa1 siRNA. The cells were treated with osteogenic medium and BMP2 as before, and expression of Cbfa1, Osterix, SM22α, αSMA and SM-MHC was determined by immunoblotting. The depletion of Cbfa1 did not affect expression of SM22α or αSMA, and depletion of SM22α did not affect expression of Cbfa1 or Osterix (Figure 8B). No expression of SM-MHC was detected in any of the samples, suggesting that the cells do not undergo late SMC differentiation. The results suggested that expression of SM22α is not required for the ECs to undergo osteogenic differentiation.

DISCUSSION

In this report, we demonstrate that the vascular endothelium acts as a source of multipotent cells that may contribute to vascular calcification in states of high BMP activity, such as lack of the BMP-inhibitor MGP [17] and hyperglycemia [9]. Vascular calcification could therefore be considered an acquired stem cell disorder in these settings.

It has previously been shown that BMP4 binds to the ALK2 receptor, which allows for EndMT and the generation of cells that are able to undergo osteoinduction. FOP, characterized by ectopic soft tissue calcification, is caused by mutations in ALK2 that render the receptor constitutively active [3]. In our study, ALK2 is activated in the aortic endothelium of both $Mgp^{-/-}$ and the $Ins2^{Akita/+}$ mice, in the $Mgp^{-/-}$mice due to lack of BMP4 inhibition, and in the $Ins2^{Akita/+}$ mice due to induction of BMP4 and ALK2 [9, 17]. However, the resulting EndMT and multipotent cells appear to be restricted to the artery wall in these mice [9, 19], whereas FOP lesions are found outside the major vessels [3, 4, 34]. In the diabetic mice, the increase in BMP4/ALK2 activity overwhelms the available BMP inhibition, which

can be enhanced by increasing the expression of MGP through a transgene [9]. The increase in MGP led to a limitation of vascular calcification in the previous study [9], and was consistent with the decrease in the expression of multipotency markers seen in the current study. EndMT have also been reported in ECs derived from the mitral valve leaflets [6], and in HAECs *in vitro* [7], which together with our data support an important role for the endothelium in the development of cardiovascular calcification.

Mechanistically, BMP4 is known to induce expression of MGP in ECs [15], which provides negative feedback inhibition for BMP2 and 4 [16], and regulates BMP-induced events in the vascular wall [8, 9]. Such activities may include the promotion of multipotency, EC proliferation and differentiation, and osteogenic induction [13, 17, 35–37]. BMP4 alone was sufficient to stimulate osteogenic induction in human umbilical vein ECs and human cutaneous microvascular ECs [3], whereas MGP depletion, preferably in combination with BMP treatment, induced osteogenic differentiation in the HAECs in our experiments. The optimal balance between BMP4 treatment and MGP depletion required for osteoinduction may vary between different types of cultured ECs, and is not yet fully elucidated.

We used the *Tie2-Gfp* transgene for endothelial lineage tracing in an approach similar to that used by other investigators [3]. Expression of Tie2 and VE-cadherin, both commonly used for lineage tracing and excision in the endothelium, has been detected in small subpopulations of hematopoietic cells, and in areas of endocardial-mesenchymal transformation in the embryonic atrioventricular canal and outflow tract [38, 39]. Although it is impossible to exclude, it is less likely that hematopoietic cells, such as monocytes, would directly transition to osteoprogenitor cells in these studies, especially in the $Mgp^{-/-}$aortas where the expression of inflammatory and monocyte markers is minimal or undetectable [8]. Furthermore, even if the exclusion of CD45+ cells prior to FACS analysis of aortic cells from $Mgp^{-/-}$ and $Ins2^{Akita/+}$ may have removed a small number of CD45+CD31+ leukocytic cells, 20–30% of the analyzed cells still co-expressed CD31 and Cbfa1 or Sox2. Finally, our lineage tracing was accompanied by co-staining of EC and multipotency or osteogenic markers, which gave similar results, supporting our conclusions. Overall, this supports that osteogenic cells can be derived from the vascular endothelium.

The goal of our study is to determine whether ECs can give rise to osteogenic cells. Thus, an analysis of the origin of the ECs is beyond the scope of this study. The ECs may be derived locally or from EC progenitors from the bone marrow. Indeed, Cho et al. recently showed that bone-marrow derived cells easily gained access to atherosclerotic aortic wall in $Apoe^{-/-}$ mice [40], and Naik et al. estimated that bone marrow-derived cells account for ~20% of Cbfa1-positive cells in the calcified atherosclerotic vessels of $Apoe^{-/-}$ mice [41]. However, none of these investigators explored whether the bone marrow-derived cells differentiated into ECs or EC-like cells.

It has been proposed that osteoblastic cells in the media are derived from SMCs based on lineage tracing using *SM22α-LacZ* transgenic mice and *Cbfa1 (Runx2)* deletion in *SM22α*-expressing cells [2, 30]. The osteoblastic cells could also be derived from a new type of multipotent vascular stem cells recently identified in the blood vessel wall, which become proliferative and undergo SMC and osteochondrogenic cell differentiation after vascular injury [42]. In our studies, MGP-depletion in the HAECs induced expression of both early SMC markers (SM22α and αSMA) and osteogenic markers (Cbfa1 and Osterix). However, no expression of the late SMC marker SM-MHC was detected. Furthermore, depletion of both MGP and SM22α still allowed for the induction of the osteogenic markers, suggesting that SM22α is not required for osteoinduction in these cells. Thus, it is possible that osteoprogenitor cells derived from the endothelium do not express SM22α and would not be detected when the SM22α–promoter is used for lineage tracing. Alternatively, SM22α–

expressing cells in the vascular wall, known to contribute to vascular calcification, may be the result of prior EndMT in the vascular endothelium.

Induction of multipotency by BMP in endothelium is an important physiological mechanism during development and after injury. Such activation would provide a local source of stem cells that could promote growth or healing of the vasculature itself, or tissue-specific cell differentiation depending on local cues. It would be consistent with the concept of "stemness" being a function of the local context [43]. Overall, our data support that diseased endothelium with excess BMP activity may contribute osteoprogenitor cells to vascular calcification.

Supplementary Material

Refer to Web version on PubMed Central for supplementary material.

Acknowledgments

SOURCES OF FUNDING

Funding was provided in part by NIH grants HL30568, HL81397, HL112839, and NS79353, ZDK1 GRB-J O1, and the American Heart Association.

Electron microscopy was performed under supervision of Sirus A. Kohan at the Electron Microscopy Services Center of UCLA Brain Research Institute.

Nonstandard Abbreviations and Acronyms

ALK	Activin-like kinase receptor
ALP	Alkaline phosphatase
BMP	Bone morphogenetic protein
Cbfa1	Core binding factor alpha 1
CD	Cluster of differentiation
EndMT	Endothelial-mesenchymal transition
Flk-1	Fetal liver kinase 1
FOP	Fibrodysplasia ossificans progressiva
Gla	Gamma-carboxyglutamic acid
HAEC	Human aortic endothelial cells
IgG	Immunoglobulin G
MGP	Matrix Gla protein
pSMAD	Phosphorylated SMAD
SMAD	Homolog of the drosophila protein, mothers against decapentaplegic (MAD) and the *C. elegans* protein SMA
SMC	Smooth muscle cells
SSEA	Stage-specific embryonic antigen
tg	transgenic
Tie2	Tyrosine-protein kinase receptor TIE-2

vWF	von Willebrand factor
wt	wild type

References

1. Sage AP, Tintut Y, Demer LL. Regulatory mechanisms in vascular calcification. Nat Rev Cardiol. 2010; 7:528–536. [PubMed: 20664518]
2. Speer MY, Yang HY, Brabb T, Leaf E, Look A, Lin WL, Frutkin A, Dichek D, Giachelli CM. Smooth muscle cells give rise to osteochondrogenic precursors and chondrocytes in calcifying arteries. Circ Res. 2009; 104:733–741. [PubMed: 19197075]
3. Medici D, Shore EM, Lounev VY, Kaplan FS, Kalluri R, Olsen BR. Conversion of vascular endothelial cells into multipotent stem-like cells. Nat Med. 2010; 16:1400–1406. [PubMed: 21102460]
4. Kaplan FS, Xu M, Seemann P, Connor JM, Glaser DL, Carroll L, Delai P, Fastnacht-Urban E, Forman SJ, Gillessen-Kaesbach G, Hoover-Fong J, Koster B, Pauli RM, Reardon W, Zaidi SA, Zasloff M, Morhart R, Mundlos S, Groppe J, Shore EM. Classic and atypical fibrodysplasia ossificans progressiva (fop) phenotypes are caused by mutations in the bone morphogenetic protein (bmp) type i receptor acvr1. Hum Mutat. 2009; 30:379–390. [PubMed: 19085907]
5. Dudley AC, Khan ZA, Shih SC, Kang SY, Zwaans BM, Bischoff J, Klagsbrun M. Calcification of multipotent prostate tumor endothelium. Cancer Cell. 2008; 14:201–211. [PubMed: 18772110]
6. Wylie-Sears J, Aikawa E, Levine RA, Yang JH, Bischoff J. Mitral valve endothelial cells with osteogenic differentiation potential. Arterioscler Thromb Vasc Biol. 2011; 31:598–607. [PubMed: 21164078]
7. Tang R, Gao M, Wu M, Liu H, Zhang X, Liu B. High glucose mediates endothelial-to-chondrocyte transition in human aortic endothelial cells. Cardiovasc Diabetol. 2012; 11:113. [PubMed: 22998723]
8. Yao Y, Bennett BJ, Wang X, Rosenfeld ME, Giachelli C, Lusis AJ, Bostrom KI. Inhibition of bone morphogenetic proteins protects against atherosclerosis and vascular calcification. Circ Res. 2010; 107:485–494. [PubMed: 20576934]
9. Bostrom KI, Jumabay M, Matveyenko A, Nicholas SB, Yao Y. Activation of vascular bone morphogenetic protein signaling in diabetes mellitus. Circ Res. 2010; 108:446–457. [PubMed: 21193740]
10. Derwall M, Malhotra R, Lai CS, Beppu Y, Aikawa E, Seehra JS, Zapol WM, Bloch KD, Yu PB. Inhibition of bone morphogenetic protein signaling reduces vascular calcification and atherosclerosis. Arterioscler Thromb Vasc Biol. 2012; 32:613–622. [PubMed: 22223731]
11. Nakagawa Y, Ikeda K, Akakabe Y, Koide M, Uraoka M, Yutaka KT, Kurimoto-Nakano R, Takahashi T, Matoba S, Yamada H, Okigaki M, Matsubara H. Paracrine osteogenic signals via bone morphogenetic protein-2 accelerate the atherosclerotic intimal calcification in vivo. Arterioscler Thromb Vasc Biol. 2010; 30:1908–1915. [PubMed: 20651281]
12. Csiszar A, Lehoux S, Ungvari Z. Hemodynamic forces, vascular oxidative stress and regulation of bmp-2/4 expression. Antioxid Redox Signal. 2009; 11:1683–1697. [PubMed: 19320562]
13. Bostrom KI, Rajamannan NM, Towler DA. The regulation of valvular and vascular sclerosis by osteogenic morphogens. Circ Res. 2011; 109:564–577. [PubMed: 21852555]
14. Chang K, Weiss D, Suo J, Vega JD, Giddens D, Taylor WR, Jo H. Bone morphogenic protein antagonists are coexpressed with bone morphogenic protein 4 in endothelial cells exposed to unstable flow in vitro in mouse aortas and in human coronary arteries: Role of bone morphogenic protein antagonists in inflammation and atherosclerosis. Circulation. 2007; 116:1258–1266. [PubMed: 17785623]
15. Yao Y, Zebboudj AF, Shao E, Perez M, Bostrom K. Regulation of bone morphogenetic protein-4 by matrix gla protein in vascular endothelial cells involves activin-like kinase receptor 1. J Biol Chem. 2006; 281:33921–33930. [PubMed: 16950789]

16. Yao Y, Shahbazian A, Bostrom KI. Proline and gamma-carboxylated glutamate residues in matrix gla protein are critical for binding of bone morphogenetic protein-4. Circ Res. 2008; 102:1065–1074. [PubMed: 18369157]

17. Yao Y, Jumabay M, Wang A, Bostrom KI. Matrix gla protein deficiency causes arteriovenous malformations in mice. J Clin Invest. 2011; 121:2993–3004. [PubMed: 21765215]

18. Wallin R, Cain D, Hutson SM, Sane DC, Loeser R. Modulation of the binding of matrix gla protein (mgp) to bone morphogenetic protein-2 (bmp-2). Thromb Haemost. 2000; 84:1039–1044. [PubMed: 11154111]

19. Luo G, Ducy P, McKee MD, Pinero GJ, Loyer E, Behringer RR, Karsenty G. Spontaneous calcification of arteries and cartilage in mice lacking matrix gla protein. Nature. 1997; 386:78–81. [PubMed: 9052783]

20. Yoshioka M, Kayo T, Ikeda T, Koizumi A. A novel locus, mody4, distal to d7mit189 on chromosome 7 determines early-onset niddm in nonobese c57bl/6 (akita) mutant mice. Diabetes. 1997; 46:887–894. [PubMed: 9133560]

21. Breyer MD, Bottinger E, Brosius FC 3rd, Coffman TM, Harris RC, Heilig CW, Sharma K. Mouse models of diabetic nephropathy. J Am Soc Nephrol. 2005; 16:27–45. [PubMed: 15563560]

22. Yao Y, Nowak S, Yochelis A, Garfinkel A, Bostrom KI. Matrix gla protein, an inhibitory morphogen in pulmonary vascular development. J Biol Chem. 2007; 282:30131–30142. [PubMed: 17670744]

23. Motoike T, Loughna S, Perens E, Roman BL, Liao W, Chau TC, Richardson CD, Kawate T, Kuno J, Weinstein BM, Stainier DY, Sato TN. Universal gfp reporter for the study of vascular development. Genesis. 2000; 28:75–81. [PubMed: 11064424]

24. Lee H, Shi W, Tontonoz P, Wang S, Subbanagounder G, Hedrick CC, Hama S, Borromeo C, Evans RM, Berliner JA, Nagy L. Role for peroxisome proliferator-activated receptor alpha in oxidized phospholipid-induced synthesis of monocyte chemotactic protein-1 and interleukin-8 by endothelial cells. Circ Res. 2000; 87:516–521. [PubMed: 10988245]

25. Bostrom K, Tsao D, Shen S, Wang Y, Demer LL. Matrix gla protein modulates differentiation induced by bone morphogenetic protein-2 in c3h10t1/2 cells. J Biol Chem. 2001; 276:14044–14052. [PubMed: 11278388]

26. Yao Y, Bennett BJ, Wang X, Rosenfeld ME, Giachelli C, Lusis AJ, Bostrom KI. Inhibition of bone morphogenetic proteins protects against atherosclerosis and vascular calcification. Circ Res. 2010; 107:485–494. [PubMed: 20576934]

27. Hartley CJ, Taffet GE, Reddy AK, Entman ML, Michael LH. Noninvasive cardiovascular phenotyping in mice. ILAR J. 2002; 43:147–158. [PubMed: 12105382]

28. Basu R, Oudit GY, Wang X, Zhang L, Ussher JR, Lopaschuk GD, Kassiri Z. Type 1 diabetic cardiomyopathy in the akita (ins2wt/c96y) mouse model is characterized by lipotoxicity and diastolic dysfunction with preserved systolic function. Am J Physiol Heart Circ Physiol. 2009; 297:H2096–2108. [PubMed: 19801494]

29. Nasrallah R, Xiong H, Hebert RL. Renal prostaglandin e2 receptor (ep) expression profile is altered in streptozotocin and b6-ins2akita type i diabetic mice. Am J Physiol Renal Physiol. 2007; 292:F278–284. [PubMed: 16954344]

30. Sun Y, Byon CH, Yuan K, Chen J, Mao X, Heath JM, Javed A, Zhang K, Anderson PG, Chen Y. Smooth muscle cell-specific runx2 deficiency inhibits vascular calcification. Circ Res. 2012; 111:543–552. [PubMed: 22773442]

31. Kokudo T, Suzuki Y, Yoshimatsu Y, Yamazaki T, Watabe T, Miyazono K. Snail is required for tgfbeta-induced endothelial-mesenchymal transition of embryonic stem cell-derived endothelial cells. J Cell Sci. 2008; 121:3317–3324. [PubMed: 18796538]

32. Wirz W, Antoine M, Tag CG, Gressner AM, Korff T, Hellerbrand C, Kiefer P. Hepatic stellate cells display a functional vascular smooth muscle cell phenotype in a three-dimensional co-culture model with endothelial cells. Differentiation. 2008; 76:784–794. [PubMed: 18177423]

33. Ding R, Darland DC, Parmacek MS, D'Amore PA. Endothelial-mesenchymal interactions in vitro reveal molecular mechanisms of smooth muscle/pericyte differentiation. Stem Cells Dev. 2004; 13:509–520. [PubMed: 15588508]

34. el-Labban NG, Hopper C, Barber P. Ultrastructural finding of vascular degeneration in fibrodysplasia ossificans progressiva (fop). J Oral Pathol Med. 1995; 24:125–129. [PubMed: 7776264]
35. Vicente Lopez MA, Vazquez Garcia MN, Entrena A, Olmedillas Lopez S, Garcia-Arranz M, Garcia-Olmo D, Zapata A. Low doses of bone morphogenetic protein 4 increase the survival of human adipose-derived stem cells maintaining their stemness and multipotency. Stem Cells Dev. 2010
36. Yang L, Soonpaa MH, Adler ED, Roepke TK, Kattman SJ, Kennedy M, Henckaerts E, Bonham K, Abbott GW, Linden RM, Field LJ, Keller GM. Human cardiovascular progenitor cells develop from a kdr+ embryonic-stem-cell-derived population. Nature. 2008; 453:524–528. [PubMed: 18432194]
37. Boyd NL, Dhara SK, Rekaya R, Godbey EA, Hasneen K, Rao RR, West FD 3rd, Gerwe BA, Stice SL. Bmp4 promotes formation of primitive vascular networks in human embryonic stem cell-derived embryoid bodies. Exp Biol Med. 2007; 232:833–843.
38. Alva JA, Zovein AC, Monvoisin A, Murphy T, Salazar A, Harvey NL, Carmeliet P, Iruela-Arispe ML. Ve-cadherin-cre-recombinase transgenic mouse: A tool for lineage analysis and gene deletion in endothelial cells. Dev Dyn. 2006; 235:759–767. [PubMed: 16450386]
39. Kisanuki YY, Hammer RE, Miyazaki J, Williams SC, Richardson JA, Yanagisawa M. Tie2-cre transgenic mice: A new model for endothelial cell-lineage analysis in vivo. Dev Biol. 2001; 230:230–242. [PubMed: 11161575]
40. Cho HJ, Lee HJ, Song MK, Seo JY, Bae YH, Kim JY, Lee HY, Lee W, Koo BK, Oh BH, Park YB, Kim HS. Vascular calcifying progenitor cells possess bidirectional differentiation potentials. PLoS Biol. 2013; 11:e1001534. [PubMed: 23585735]
41. Naik V, Leaf EM, Hu JH, Yang HY, Nguyen NB, Giachelli CM, Speer MY. Sources of cells that contribute to atherosclerotic intimal calcification: An in vivo genetic fate mapping study. Cardiovasc Res. 2012; 94:545–554. [PubMed: 22436847]
42. Tang Z, Wang A, Yuan F, Yan Z, Liu B, Chu JS, Helms JA, Li S. Differentiation of multipotent vascular stem cells contributes to vascular diseases. Nat Commun. 2012; 3:875. [PubMed: 22673902]
43. Bostrom KI, Garfinkel A, Yao Y, Jumabay M. Concise review: Applying stem cell biology to vascular structures. Stem Cells. 2012; 30:386–391. [PubMed: 22232064]

Novelty and Significance

What Is Known?

- Vascular calcification is a frequent complication of diabetic vasculopathy and atherosclerosis.
- Vascular calcification is a regulated process driven by osteochondrogenic differentiation of vascular medial cells.
- Bone morphogenetic proteins (BMPs) promote vascular calcification, whereas Matrix Gla protein (MGP), a BMP inhibitor, protects against calcification.

What New Information Does This Article Contribute?

- The vascular endothelium contributes osteoprogenitor cells to vascular calcification in diabetic mice and MGP-null mice.
- Enhanced BMP signaling in endothelial cells (due to the MGP knockout or enhanced BMP expression in diabetes) results in endothelial-mesenchymal transitions and the emergence of multipotent cells, which are susceptible to bone induction.
- MGP prevents the generation of multipotent cells from the vascular endothelium.

Vascular calcification is a regulated process that involves osteoprogenitor cells and frequently complicates vascular disease. Nevertheless, the role of the vascular endothelium in this process is poorly understood. We report that the endothelium can directly contribute osteoprogenitor cells to the vascular calcification. Using mouse models and cultured endothelial cells, we demonstrate that increased BMP signaling, either due to lack of the BMP-inhibitor MGP or enhanced BMP expression, stimulates the endothelial-mesenchymal transition and the emergence of multipotent cells. These multipotent cells are susceptible to bone induction in the setting of disorders such as diabetic vasculopathy. These findings identify the endothelium as a new source of osteoprogenitor cells in vascular calcification and suggest that multipotency or “stemness” in the vascular wall is a function of the local context.

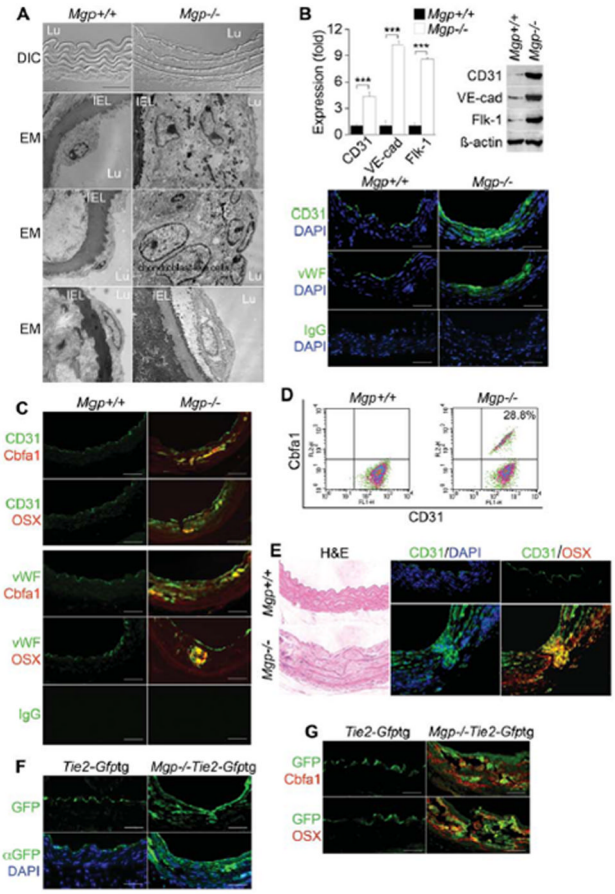

Figure 1. Endothelium contributes cells to aortic calcification of Mgp$^{-/-}$ mice

(A) Aortic wall (confocal microscopy, top 2 panels), and aortic endothelium () from wild type (*Mgp*$^{+/+}$) and *Mgp*$^{-/-}$ mice. DIC: differential interference contrast. EM: electron microscopy. Magnification for EM, 3.7 ×10^3. (B) Aortic expression of endothelial markers CD31, VE-cadherin (VE-cad), Flk-1 and vWF in *Mgp*$^{+/+}$ and *Mgp*$^{-/-}$ mice determined by real-time PCR, immunoblotting and immunostaining. ***, p <0.001. (C) Immunostaining of aortic tissues from *Mgp*$^{+/+}$ and *Mgp*$^{-/-}$ mice showed co-expression of endothelial markers CD31 (top) and vWF (bottom) and osteogenic markers Cbfa1 and Osterix (OSX) in the *Mgp*$^{-/-}$mice. (D) Co-expression of CD31 and Cbfa1 in enzymatically dispersed CD45-negative aortic cells from *Mgp*$^{+/+}$ and *Mgp*$^{-/-}$ mice, as determined by FACS. (E) Cells co-expressing CD31 and Osterix that have penetrated into the medial layer in *Mgp*$^{-/-}$ aorta. (F) Visualization of GFP (top) and immunostaining with anti-GFP antibodies (bottom) in aortic tissue of *Tie2-Gfp*tg and *Mgp*$^{-/-}$*;Tie2-Gfp*tg mice. (G) Immunostaining of aortic tissues from *Tie2-Gfp*tg and *Mgp*$^{-/-}$*;Tie2-Gfp*tg mice showed co-expression of GFP with Cbfa1 and OSX in the Mgp$^{-/-}$;*Tie2-Gfp*tg mice. Scale bars, 100 μm. DAPI (blue) was used to visualize nuclei. Non-specific IgG control showed no staining. Vessel lumen faces upwards in the photos unless otherwise indicated.

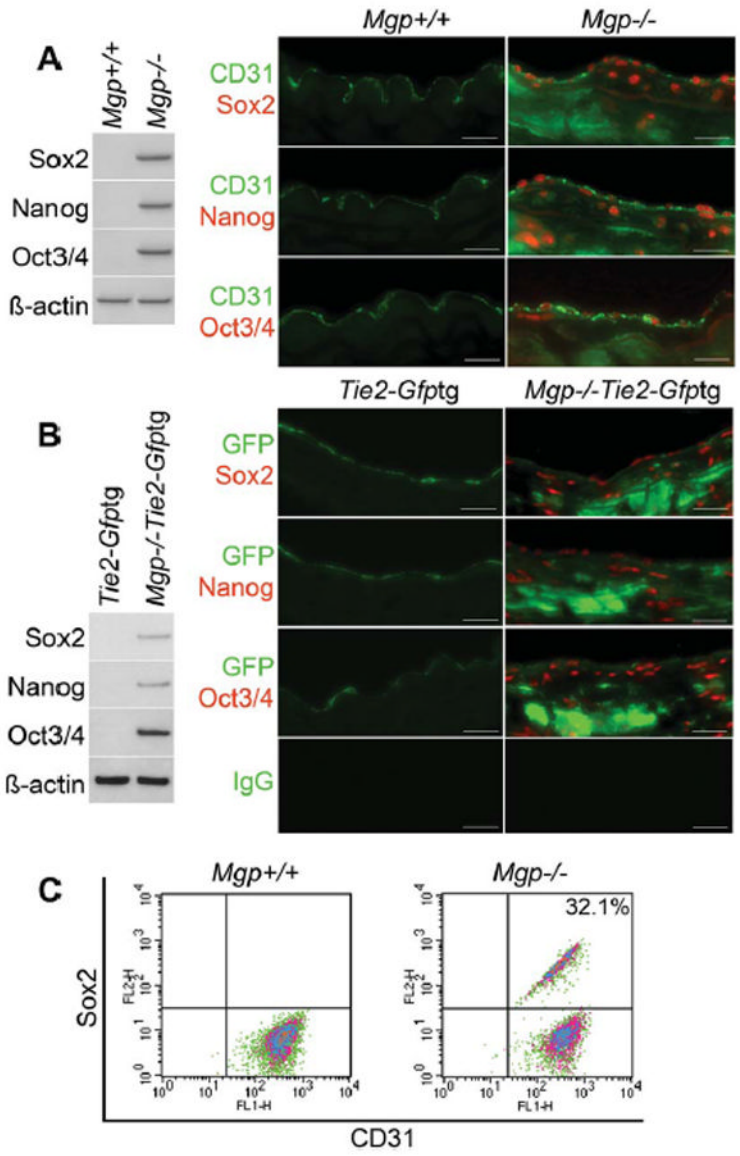

Figure 2. Multipotent marker expression in Mgp$^{-/-}$ and Mgp$^{-/-}$;Tie2-Gfptg endothelium

(A) Aortic expression of Sox2, Nanog and Oct3/4 in *Mgp*$^{+/+}$ and *Mgp*$^{-/-}$ mice detected by immunoblotting (left) and immunostaining (right). β-actin was used as control. (B) Aortic expression of Sox2, Nanog and Oct3/4 in *Tie2-Gfp*tg and *Mgp*$^{-/-}$*;Tie2-Gfp*tgmice determined by immunoblotting (left) and immunostaining (right). β-actin was used as control. (C) Co-expression of CD31 and Sox2 in enzymatically dispersed CD45-negative aortic cells from *Mgp*$^{+/+}$ and *Mgp*$^{-/-}$ mice, as determined by FACS. Scale bars, 50 μm. Non-specific IgG control showed no staining. Vessel lumen faces upwards in the photos.

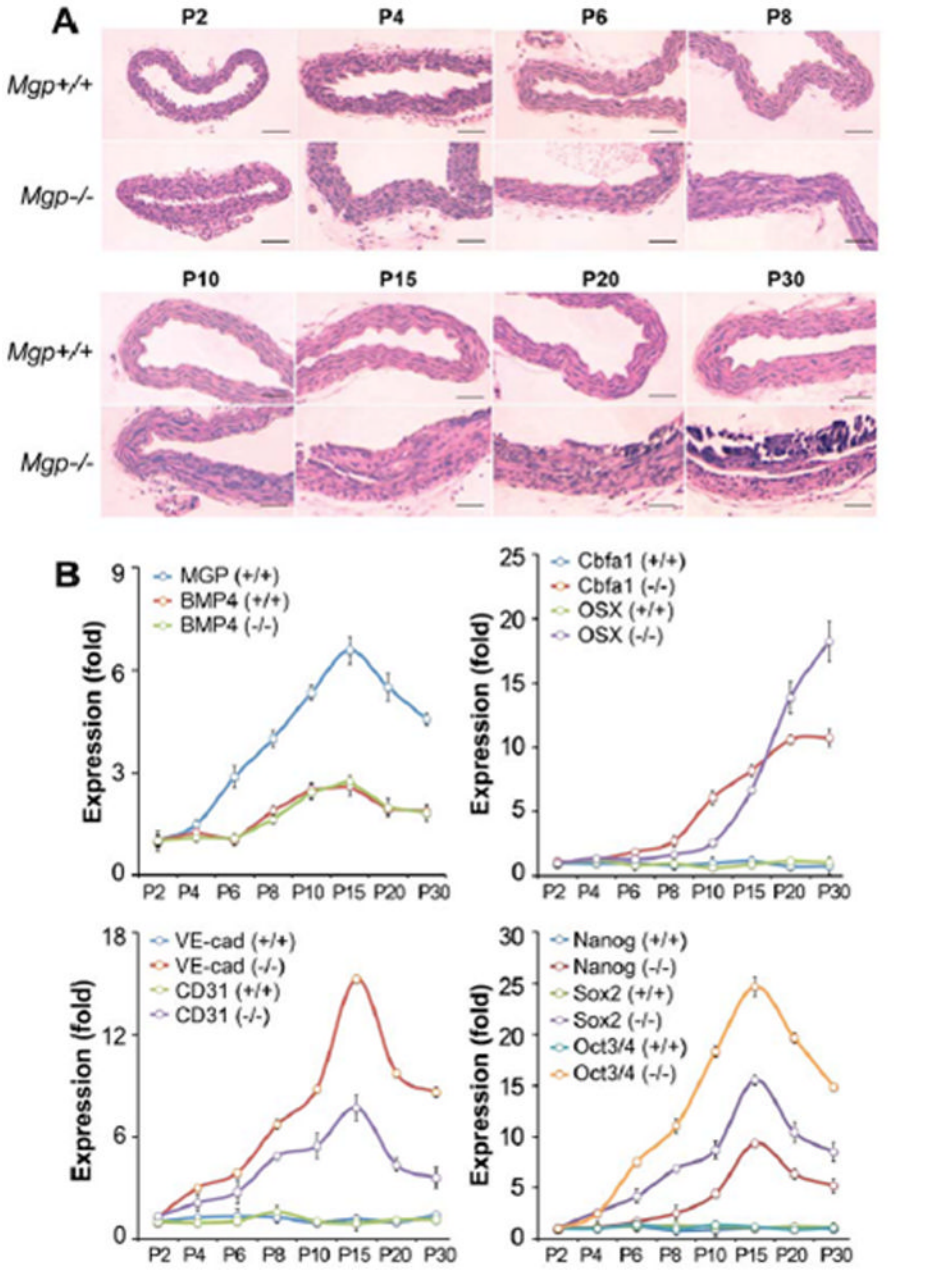

Figure 3. Time course of aortic changes in Mgp$^{-/-}$ mouse aorta

(A) Aortas were collected between postnatal day (P) 2–30 from *Mgp*$^{+/+}$ and *Mgp*$^{-/-}$ mice as indicated, and stained with H&E. (B) Time course of aortic expression in *Mgp*$^{+/+}$ and *Mgp*$^{-/-}$ aorta (P2–30) of MGP, BMP4, EC markers VE-cadherin (VE-cad) and CD31, osteogenic markers Cbfa1 and Osterix (OSX), and multipotency markers Nanog, Sox2 and Oct3/4. The expression was compared to that on P2. Scale bars, 100 μm.

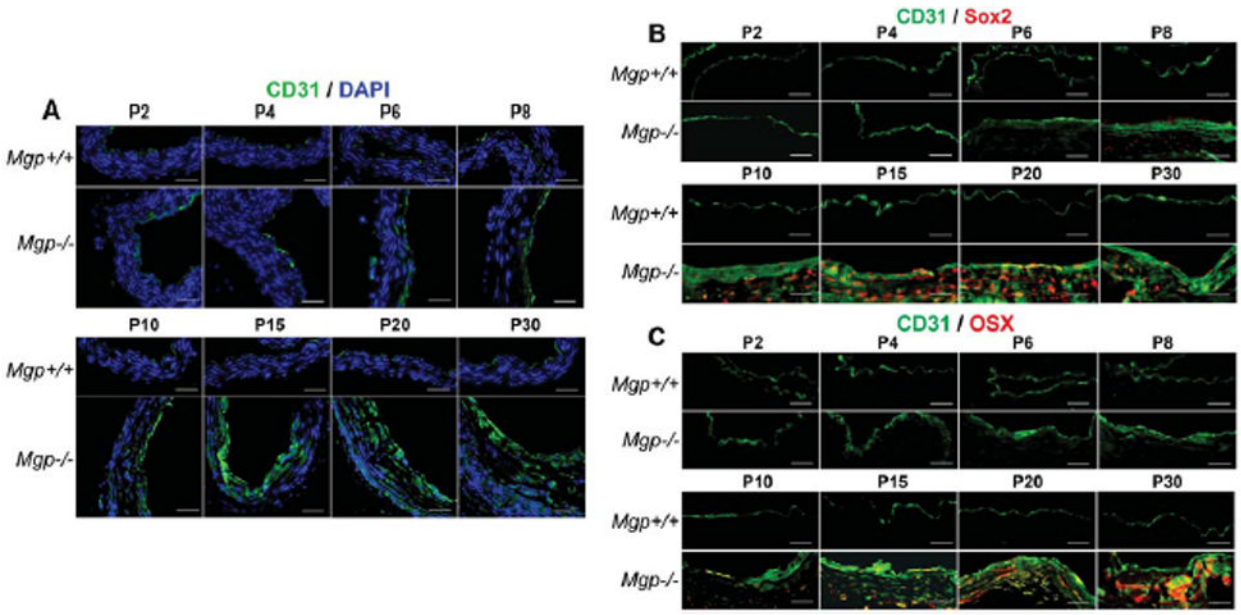

Figure 4. Time course of aortic changes in Mgp$^{-/-}$ mouse aorta

(A–C) Aortas were collected between postnatal day (P) 2–30 from *Mgp*$^{+/+}$ and *Mgp*$^{-/-}$ mice as indicated. They were immunostained for (A) CD31, (B) co-stained for CD31 and Sox2, and (C) co-stained for CD31 and Osterix (OSX). DAPI (blue) was used to visualize nuclei. Scale bars, 100 μm. DAPI (blue) was used to visualize nuclei. Vessel lumen faces upwards or to the right in the photos.

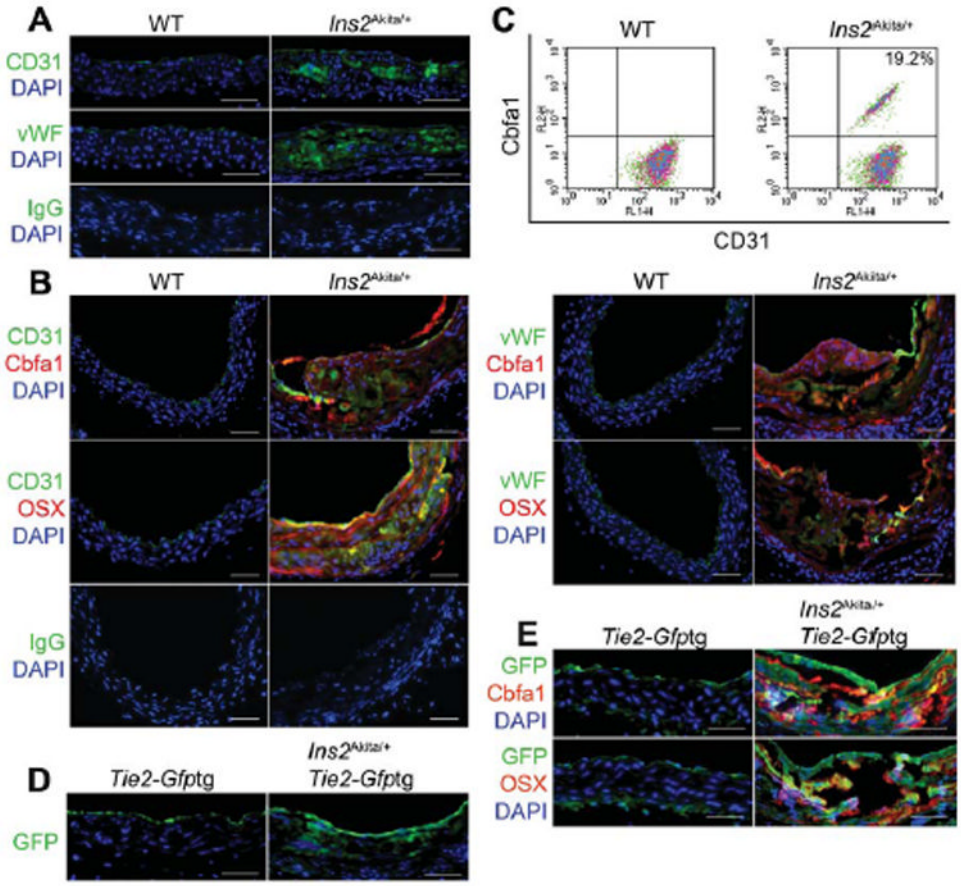

Figure 5. Endothelium contributes cells to aortic calcification of Ins2$^{Akita/+}$ mice

(A) Aortic expression of endothelial markers CD31 and vWF in *Ins2$^{Akita/+}$* mice visualized by immunostaining. (B) Immunostaining of aortic tissues from wild type (WT) and *Ins2$^{Akita/+}$* mice showed co-expression of endothelial markers CD31 (left) and vWF (right) and osteogenic markers Cbfa1 and Osterix (OSX) in the *Ins2$^{Akita/+}$* mice. (C) Co-expression of CD31 and Cbfa1 in enzymatically dispersed aortic cells from WT and *Ins2$^{Akita/+}$ mice*, as determined by FACS. (D) Aortic expression of GFP in *Tie2-Gfp*tg and *Ins2$^{Akita/+}$;Tie2-Gfp*tg mice by immunostaining with anti-GFP antibodies. (E) Immunostaining of aortic tissues from *Tie2-Gfp*tg and *Ins2$^{Akita/+}$;Tie2-Gfp*tg mice showed co-expression of GFP with Cbfa1 and OSX in the *Ins2$^{Akita/+}$;Tie2-Gfp*tg mice. Scale bars, 100 μm. DAPI (blue) was used to visualize nuclei. Non-specific IgG control showed no staining. Vessel lumen faces upwards in the photos.

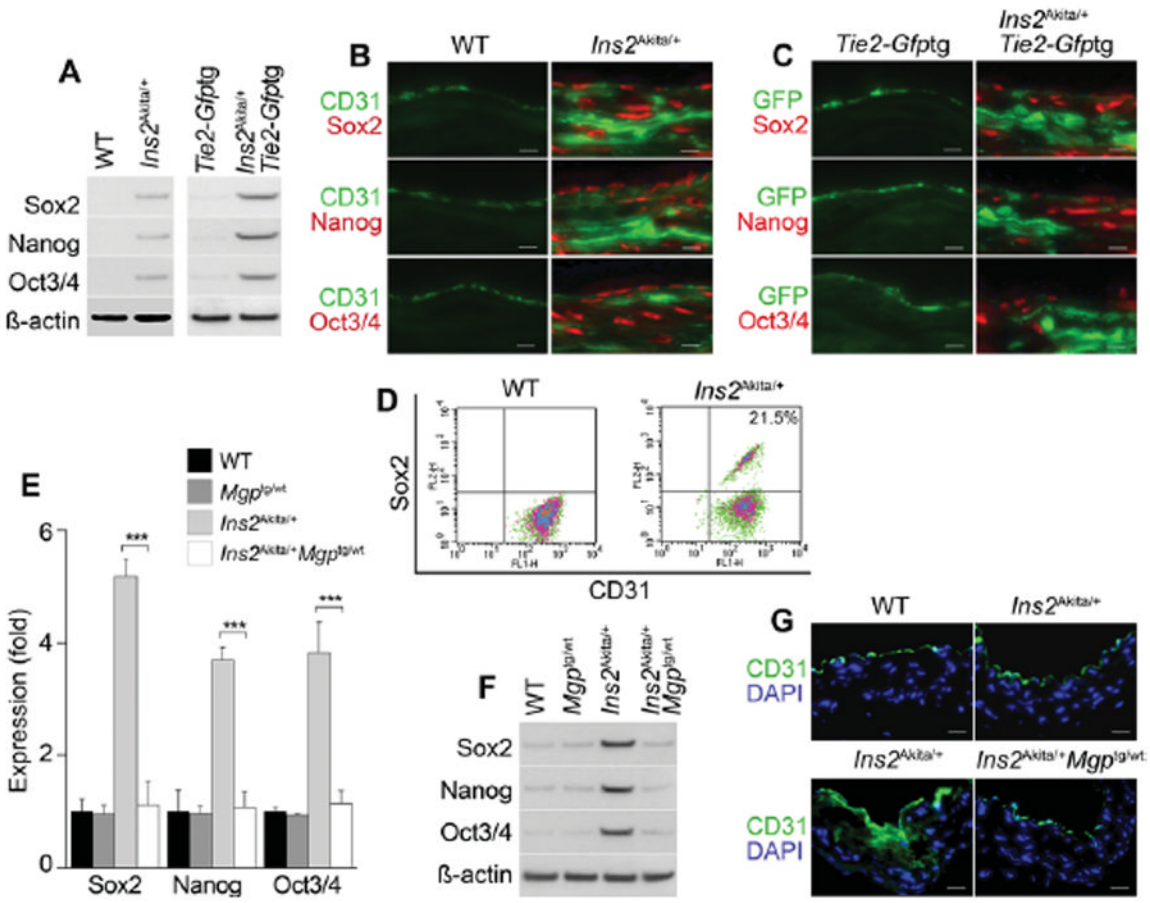

Figure 6. Endothelial origin of multipotent cells in aortas of diabetic Ins2$^{Akita/+}$ mice

(A) Aortic expression of Sox2, Nanog and Oct3/4 in wild type (WT), *Ins2$^{Akita/+}$*, *Ins2$^{Akita/+}$;Tie2-Gfp*tg and *Ins2$^{Akita/+}$;Tie2-Gfp*tg mice. β-actin was used as control. (B) Co-expression of CD31 with Sox2, Nanog and Oct3/4 in aortas of *Ins2$^{Akita/+}$* mice detected by immunostaining. (C) Co-expression of GFP with Sox2, Nanog and Oct3/4 in aortas of *Tie2-Gfp*tg and *Ins2$^{Akita/+}$;Tie2-Gfp*tg mice detected by immunostaining. (D) Co-expression of CD31 and Sox2 in enzymatically dispersed CD45-negative aortic cells from WT and *Ins2$^{Akita/+}$ mice*, as determined by FACS. (E–G) Enhanced MGP expression limits aortic expression of Sox2, Nanog and Oct3/4 in *Ins2$^{Akita/+}$* mice, as determined by (E) real-time PCR, (F) immunoblotting (β-actin was used as control), and (G) immunostaining in WT, *Mgp$^{tg/wt}$*, *Ins2$^{Akita/+}$*, and *Ins2$^{Akita/+}$;Mgp$^{tg/wt}$* mice. Scale bars, 50 μm. DAPI (blue) was used to visualize nuclei. Vessel lumen faces upwards in the photos.

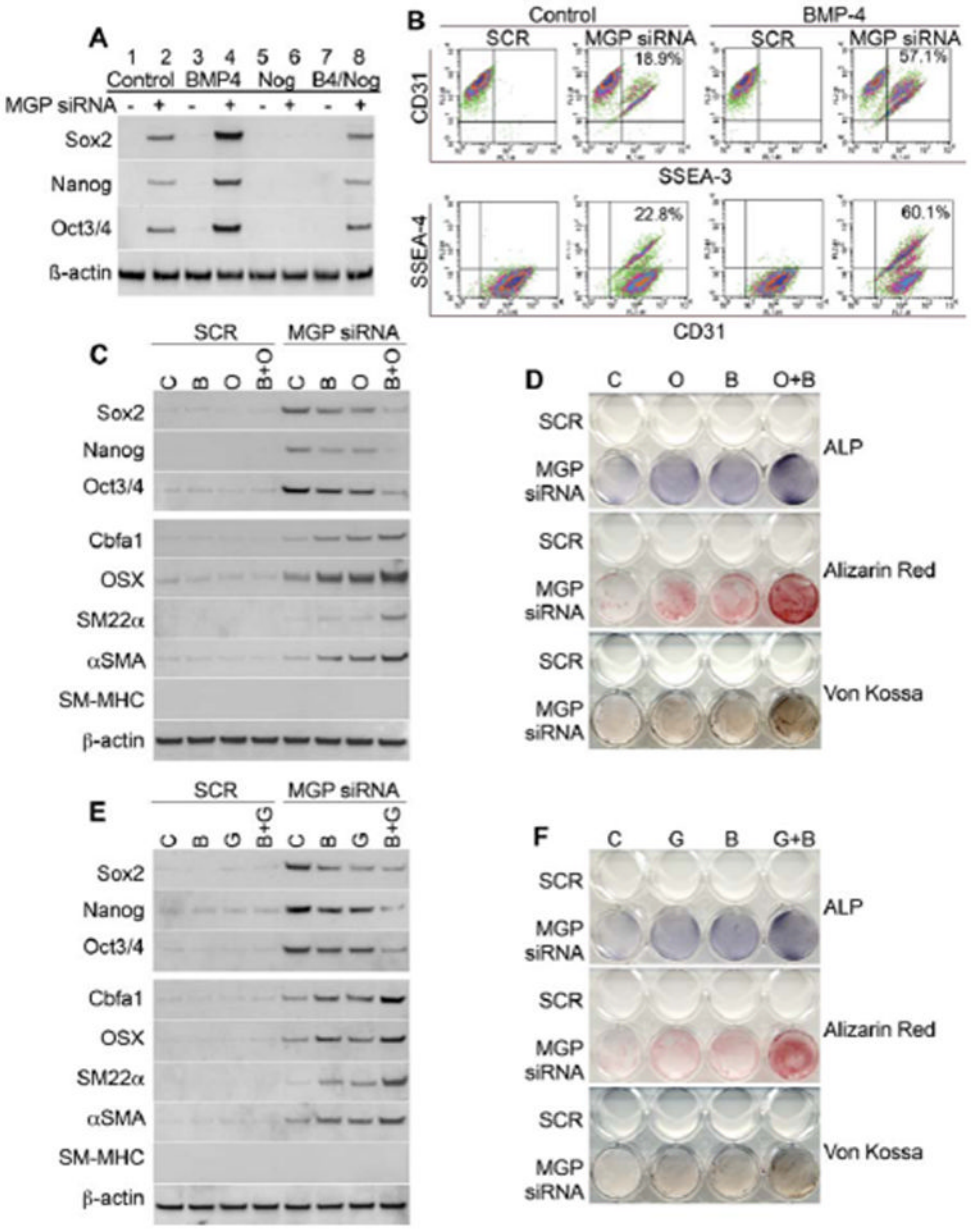

Figure 7. Depletion of MGP allows for multipotency and osteoinduction in human aortic endothelial cells (HAECs)

(A) Expression of multipotent markers Sox2, Nanog and Oct3/4 in HAECs after transfection of scrambled control siRNA (SCR) or MGP siRNA only (lane 1, 2), siRNA transfection with BMP4 treatment (lane 3, 4), siRNA transfection with Noggin treatment (lane 5, 6), or siRNA transfection with BMP4 and Noggin treatment (lane 7, 8), as determined by immunoblotting. (B) Co-expression of CD31 and SSEA-3, or CD31 and SSEA-4 after transfection of scrambled control siRNA or MGP siRNA without additional treatment (left), and with BMP4 treatment (right), as determined by FACS analysis. (C) Expression of multipotent markers Sox2, Nanog and Oct3/4, osteogenic markers Cbfa1, Osterix (OSX), early SMC markers SM22α, α-SM actin (αSMA), and late SMC marker SM-myosin heavy chain (SM-MHC) (top) after transfection of scrambled control siRNA or MGP siRNA and treatment with control (C), BMP2 (B), osteogenic media (O) or both (B+O), as determined

by immunoblotting. (D) Staining for alkaline phosphatase (ALP), and mineral (Alizarin Red and Von Kossa staining) in HAECS treated as described in (c). (E) Expression of multipotent markers Sox2, Nanog and Oct3/4, osteogenic markers Cbfa1, OSX, SM22α, αSMA, and SM-MHC (top) after transfection of scrambled control siRNA or MGP siRNA and treatment with control (C), BMP2 (B), high glucose medium (G) or both (B+G), as determined by immunoblotting. (F) Staining for ALP and mineral in HAECS treated as described in (E).

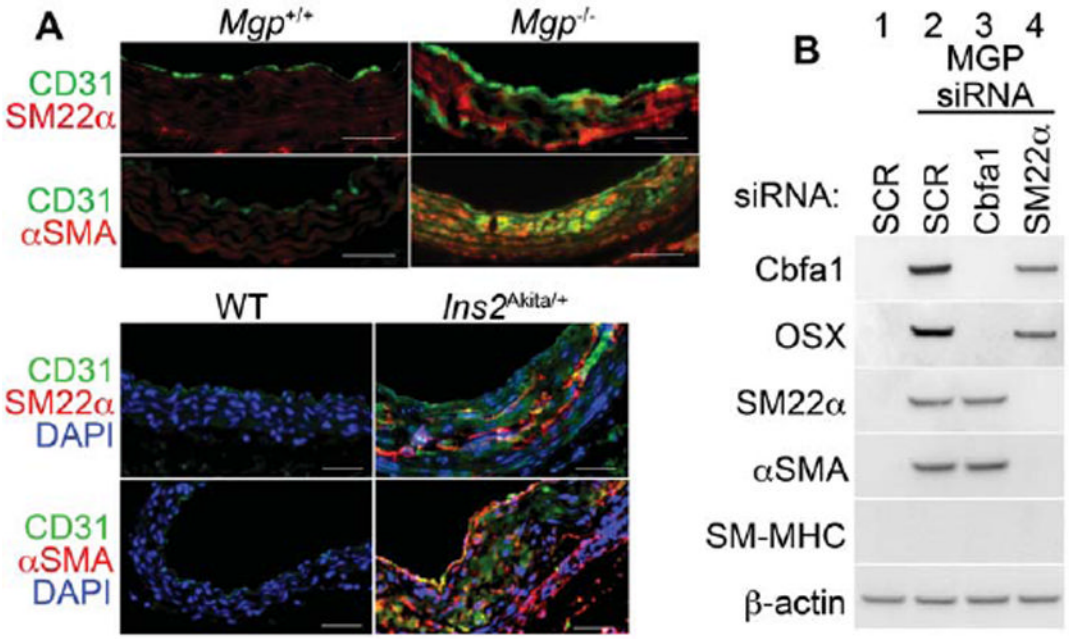

Figure 8. Osteoinduction in MGP-depleted human aortic endothelial cells does not depend on SM22α expression

(A) (Top) Immunostaining of aortic tissues from $Mgp^{+/+}$ and $Mgp^{-/-}$ mice showed co-expression of endothelial marker CD31 and early SMC markers SM22α and αSMA in the $Mgp^{-/-}$ mice. (Bottom) Immunostaining of aortic tissues from wild type (WT) and $Ins2^{Akita/+}$ mice showed co-expression of CD31 with SM22α and αSMA in the $Ins2^{Akita/+}$ mice. Scale bars, 100 μm. (B) HAECs were transfected by scrambled control siRNA (SCR) (lane1), or Mgp siRNA with ether SCR (lane 2), Cbfa1 siRNA (lane 3), or SM22a siRNA (lane 4). Expression of Cbfa1, Osterix (OSX), SM22α, α-SM actin (αSMA), and SM-myosin heavy chain (SM-MHC) was determined by immunoblotting. β-actin was used as control. Scale bars, 100 μm. DAPI (blue) was used to visualize nuclei. Vessel lumen faces upwards in the photos.